MECHANIKA TEORETYCZNA
I STOSOWANA
Journal of Theoretical
and Applied Mechanics
2, 35, 1997

THE INTERNAL STRUCTURE OF THE COLUMN-MODE COHERENT VORTEX IN FREE AXISYMMETRIC JET

STANISŁAW DROBNIAK

JANUSZ W. ELSNER

Institute of Thermal Machinery, Technical University of Częstochowa

EL-SAYED ABOU-EL-KASSEM

Faculty of Engineering, Cairo University, Egypt

The description of the internal structure of coherent vortices existing in the initial region of a round free jet has been experimentally obtained by means of computer – aided signal processing techniques. It has been found that the coherent structures in the flow considered appear initially to be the classical potential vortices. At the next stages of structure development they are subject to complex deformations which influence the intensity of transport processes.

Key words: turbulence, coherent structures, phase averaging

Notation

D	–	exit nozzle diameter
$F(x,t)$	–	instantaneous value of any physical flow property
f	–	excitation frequency
t	–	time
U	–	instantaneous value of velocity
U_c	–	convection velocity
x, r, ϕ	–	cylindrical coordinates

δ^*, δ^{**} – displacement and momentum thicknesses of the exit shear layer, respectively
ε – turbulence intensity
Θ – the instantaneous value of temperature
v – time-dependent temperature components

Subscripts and superscripts
a – ambient conditions
f – fundamental component
o – nozzle outlet plane
$(\bar{\cdot})$ – time-mean component
$(\tilde{\cdot})$ – periodic component
$(\cdot')$ – random component.

1. Introduction

The transport processes in turbulent flows become a difficult matter when the existence of coherent structures is taken into consideration, because in this case the turbulent diffusion as a major transport mechanism is replaced with the large-scale convection. Furthermore, the research done by Elsner et al. (1993) in the field of coherent structure dynamics revealed, that the axisymmetric free jets constituted an especially interesting case of the flow characterized by the presence of multiscale motion. Among all forms of coherent structures the so-called "column-mode" (cf Crow and Champagne (1971)) plays a essential role in a round free jet, because this most frequently occuring coherent structure attains a highest amplitude of velocity fluctuations. The "column-mode" structures shed in a quasi-periodic manner are very susceptible to the external flow-excitation (provided that its frequency corresponds to the shedding one) and in this way one may apply the phase-averaging procedure to detect the organized vortices and to deduce their internal structure. Most of the experimental results available in the literature (cf Hussain and Zaman (1980)) are based on the comparison of the forced flow with the "natural" (i.e. non-excited) one, that allows one to trace the influence exerted by the organized motion upon the intensity of transport processes realized in the flow considered. There is however an evident lack of information about the internal structure of vortex as this knowledge is in most cases based on visualization experiments (cf Paschereit et al. (1992)) which can give no more than qualitative description of the vortex pattern. That is why the present

experiment consists of not only a typical comparison of forced and natural flow transport properties but also the analysis of vortex internal structure. Furthermore, a small overheat of the flow has been applied which should enable tracing of the interaction of velocity and temperature fields. The comparison of the internal vortex structure data with the information about its transport properties, should in turn enable better understanding of the role of organized structures in mixing processes realized in the turbulent flow.

2. Experimental procedure and basic flow characteristics

All the measurements have been taken in an open-circuit wind tunnel (cf El-Sayed El-Kassem (1995)) equipped with the axisymmetric contoured nozzle of $D = 0.04\,\mathrm{m}$ diameter at the constant velocity of a jet exit

$$U_o = 19.4\ \mathrm{m/s}$$

that corresponded to the Reynolds number

$$\mathrm{Re}_D = \frac{\overline{U} D}{\nu} = 4 \cdot 10^4$$

The overheating of the flowing medium (i.e. the temperature difference between the ambient Θ_a and exit air Θ_o) was kept at the constant level

$$\Delta\Theta = 40^\circ\mathrm{C}$$

According to the experience gathered during the preliminary measurements (cf Elsner et al. (1989b)) it follows that such a small overheating did not introduce any significant changes into the transport mechanisms considered, and that is why the heat could be treated as a passive quantity. As the measuring area was located in a close vicinity to the jet outlet, no distortion of the horizontal jet axis caused by buoyancy was observed. The measurements have been carried out both in the natural and forced jet and in the latter case the flow was excited at the constant pressure level of $P = 110\,\mathrm{dB}$ with a pure harmonic acoustic wave of the frequency

$$f = 214\ \mathrm{Hz}$$

which corresponded to the "column-mode" (cf Crow and Champagne (1971)) structures characterized by the value of Strouhal number equal to

$$\mathrm{St}_D = \frac{f D}{U_o} = 0.42$$

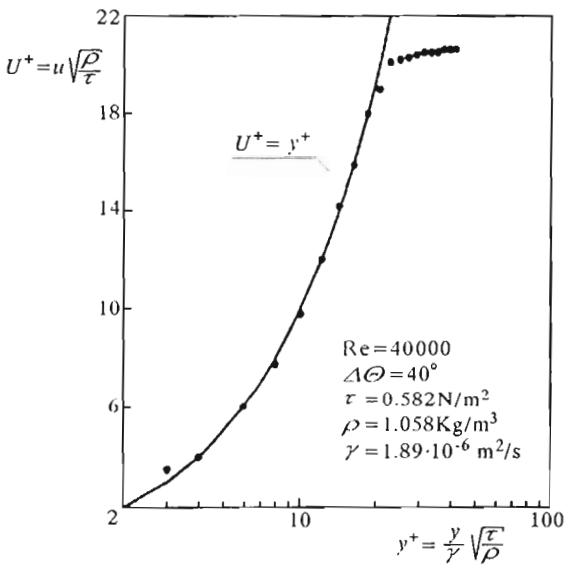

Fig. 1. Mean velocity profile in the exit shear layer in the universal coordinates U^+y^+

As can be seen in Fig.1 the mean velocity profile in exit shear layer, presented as the $U^+ = f(y^+)$ distribution, together with the information that the shape factor equals

$$\frac{\delta^*}{\delta^{**}} \cong 2.5$$

allows one to confirm the laminar character of exit boundary layer. The turbulence intensity profile measured at the jet exit (cf El-Sayed El-Kassem (1995)) reveals a flat peak located at the distance $y \approx \delta^*$ what (cf Drobniak (1986)) may be treated as an additional proof that the above statement is true.

The present experiment is characterised by a very low level of turbulence intensity outside the exit boundary layer, which was equal to

$$\varepsilon_u = \frac{\sqrt{(u'^2)}}{\overline{U}_o} \cong 0.15\%$$

as well as even lower the order of intensity of temperature fluctuations, which in the whole potential core was

$$\varepsilon_v = \frac{\sqrt{(v'^2)}}{\Delta\overline{\Theta}_o} \cong 0.1\%$$

155 measurement points distributed as shown in Fig.2 have covered the area from the jet exit up to the distance $x/D = 5$, where according to the preliminary measurements (cf Elsner et al. (1989b)), the column-mode structures reveal their coherence. The main cross-sections shown in Fig.2 were accompanied by auxiliary measuring planes which were needed to calculate more complex estimates of the vortex structure (e.g. the convection velocity U_c).

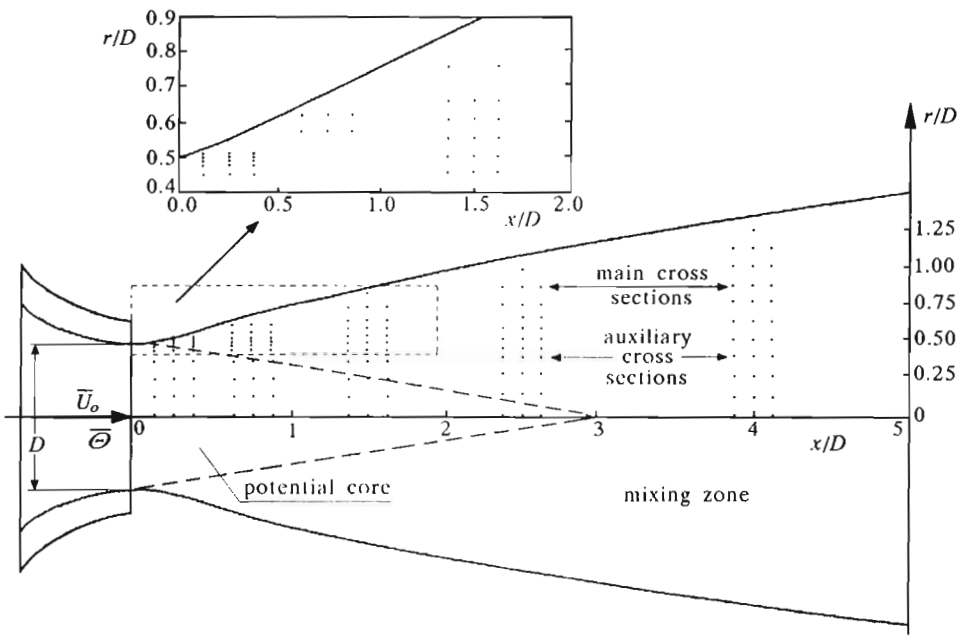

Fig. 2. Locations of the measuring points

The present experiment was based on the simultaneous measurements of three velocity components and instantaneous temperature, performed with the use of a hot-wire probe (Fig.3), supplied with the triple-wire gold-ploted DANTEC 55P91 sensor (active length of each wire equaled to 1.2 mm) and the single temperature probe DANTEC 55P31 of 0.6 mm active length.

The measuring volume occupied by the hot-wires could be approximated as a sphere of 2 mm in diameter and the proper distances between particular sensing elements ensured the avoidance of their thermal and aerodynamic interference. As shown in Fig.3, all signals from the 55P91 probe were transmitted to the Dantec 55M01 Main Units and then to the three Dantec 55M10 CTA bridges, while the sensor of 55P31 temperature probe was connected with the Dantec 55M01 Main Unit and Dantec 55M20 CCA bridge. The voltage

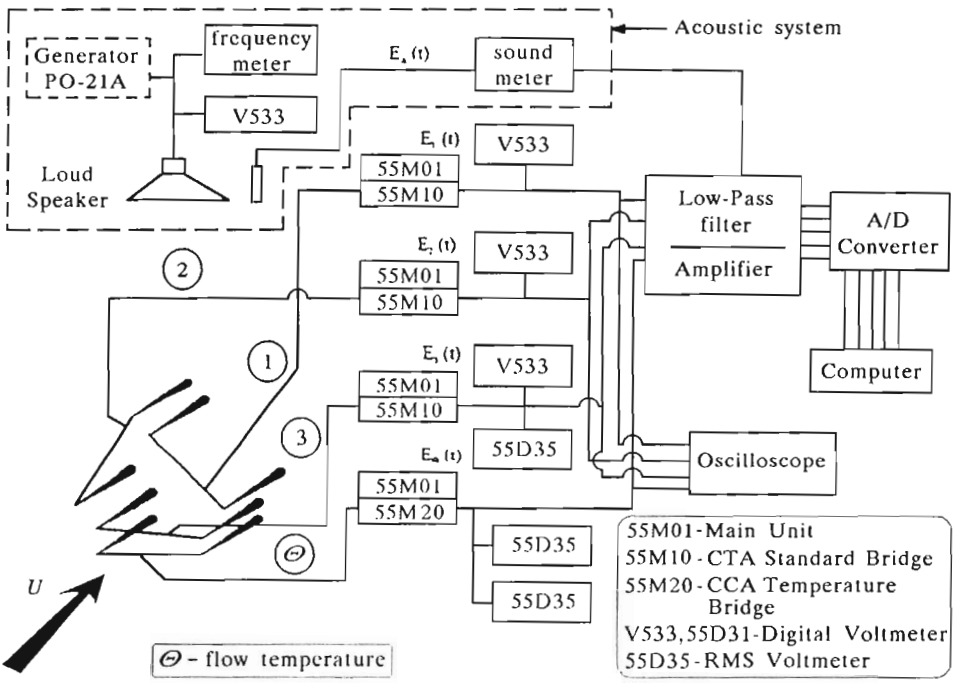

Fig. 3. Scheme of a measuring setup

signals from CTA and CCA bridges were low-pass filtered to avoid aliasing. Signals from the measuring circuits together with the acoustic pressure variation (see Fig.3) were then digitized with a 12 bit resolution, that ensured the value of quantization error below 0.012%.

The sampling frequency was equal to 14388 Hz per channel and according to the results of preliminary measurements it was sufficient to ensure a proper time resolution even for the smallest scales of the turbulent flow considered.

The data processing algorithms were based on the triple decomposition concept, i.e. each component of velocity U_i as well as the instantaneous temperature Θ were treated as the following superposition

$$U_i = \overline{U}_i + \tilde{u}_i + u_i'$$
$$\Theta = \overline{\Theta} + \tilde{v} + v' \tag{2.1}$$

Proper processing of the instantaneous time series recorded during the experiment, allowed us to obtain the characteristics of mean motion as well as the

sets of normal and shear stresses for random $\overline{U}_i$, $\overline{\Theta}$ and periodic components of flow field, i.e. $\overline{u_i' u_j'}$, $\overline{\tilde{u}_i \tilde{u}_j}$.

More details on the data acquisition and processing the reader can find in El-Sayed El-Kassem (1995).

3. The internal structure of the coherent vortex

In general, the estimates of the periodic component of flow field are time-dependent and that is why the only possible way of their analysis (cf Hussain (1986)) is to expand the phase-average of any physical flow property $\langle F(\boldsymbol{x}, t)\rangle$ into the Fourier series according to the formula

$$\langle F(\boldsymbol{x}, t)\rangle = \overline{F}(\boldsymbol{x}) + \tilde{f}(\boldsymbol{x}, t) = \overline{F}(\boldsymbol{x}) + \sum_{i=1}^{x} A_i(\boldsymbol{x}) \cos\left[2\pi \mathrm{i} \frac{t}{T} - \Phi_i(\boldsymbol{x})\right] \tag{3.1}$$

where

$\langle\cdot\rangle$	–	phase averaging operator
T	–	period of the oscillatory motion
$A_i(\boldsymbol{x}), \Phi_i(\boldsymbol{x})$	–	amplitude and phase angle respectively, of the ith component of Fourier series.

From the experience gathered so far (cf Favre-Marinet and Binder (1987), Favre-Marinet (1989)), we know that in the analysis of coherent structures four components of the series are sufficient to obtain a good representation of the $\tilde{f}(\boldsymbol{x}, t)$ component. In the case of jet-column mode, which does not reveal pairing, it is sufficient to analyze only the fundamental component $(i = 1)$ which represents the behaviour of the whole vortex (CF Drobniak (1986)).

The phase angle $\Phi_i(\boldsymbol{x})$ appearing in Eq (3.1) could be calculated with respect to the acoustic pressure reference signal, because the following codition was always fulfilled

$$\lambda_a \gg \lambda_s \tag{3.2}$$

where

λ_a	–	wavelength of the acoustic pressure reference signal
λ_s	–	wavelength of the analyzed structure.

The courses of amplitudes of the fundamental harmonics $(i = 1$ in Eq (3.1)) of the three oscillatory components of velocity $\tilde{U}_{xf}$, $\tilde{U}_{rf}$, $\tilde{U}_{\phi f}$, as well as of the periodical temperature component $\tilde{v}_f$ are presented in Fig.4 for three main cross-sections located at the distances $x = 1.5$, 2.5 and $4D$ from

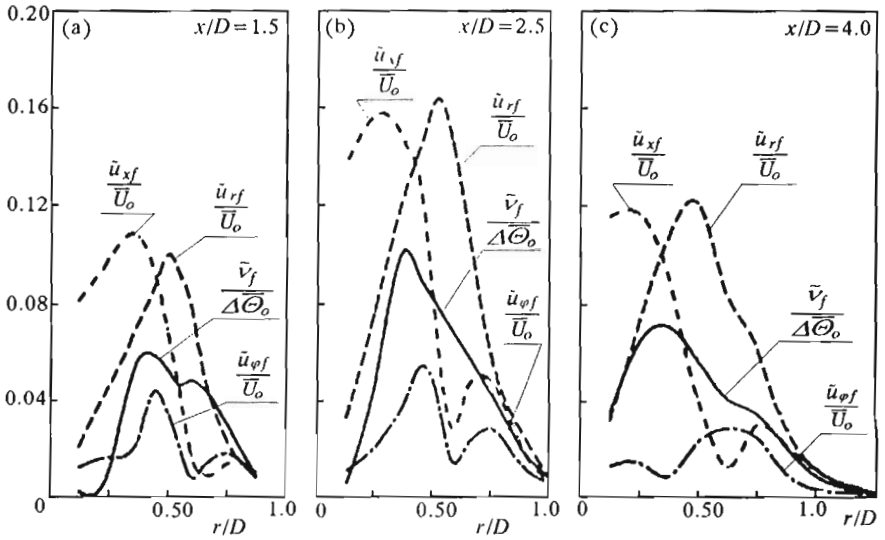

Fig. 4. Radial distributions of the fundamental harmonic amplitudes for the oscillatory components of velocity and temperature at the cross-sections: (a) – $x/D = 1.5$, (b) – $x/D = 2.5$, (c) – $x/D = 4.0$

the jet exit. It can be easily seen, that the maximum values of the longitudinal $\tilde{U}_{xf}$ and radial $\tilde{U}_{rf}$ amplitudes, respectively, are almost equal, while the circumferential $\tilde{U}_{\phi f}$ amplitude is always much smaller than the remaining ones. The fundamental amplitudes of velocity and temperature reach their maximum values at the $x/D = 2.5$ cross-sections, that confirms the previous conclusion (cf Elsner et al. (1989b)), that the column-mode structures reveal the maximum degree of coherence in this area. The asymmetry in the radial distributions of $\tilde{U}_{xf}$ with two local maxima which is most clearly visible at $x = -2.5D$ plane, results from the mutual relation between the rotation velocity inside the vortex and its convection velocity (cf Elsner et al. (1987), (1989a)). In particular, in the inner zone of the jet $(r/D < 0.5)$ convection and circumferential velocities inside the coherent structure point in the same direction (hence a higher amplitude of the inner peak), while in the outer region $(r/D > 0.5)$ the two above velocity components have opposite directions and cancel themselves. One may intuitively expect, that such a distribution of $\tilde{U}_{xf}$ may be treated as a proof, that a coherent vortex is characterized by the velocity distribution typical for a "free" vortex. The radial $\tilde{U}_{rf}$ amplitude reveals the maximum located at the line $r/D \sim 0.5$, which is the trajectory of the vortex centre. One should also notice an almost linear $\tilde{U}_{rf}$ profile in the

inner area of the jet, which is then distorted in the vicinity of the flow outer boundary.

An interesting similarity may be observed between the profiles of the $\widetilde{U}_{xf}$ and $\widetilde{U}_{\phi f}$ amplitudes at the $x/D = 1.5$ and 2.5 cross-sections, respectively (see Fig.4a,b). A possible explanation may be found in Drobniak and Elsner (1986), Drobniak (1986), where it was observed, that the column-mode vortices have been tilting in the initial jet region and this could give the circumferential periodic component which is phase-related with the $\widetilde{U}_{xf}$ amplitude.

The radial distributions of temperature oscillatory component $\widetilde{v}_f$ exhibit the behaviour depending on the location of the cross-section analyzed. In the $x/D = 1.5$ plane (Fig.4a) the $\widetilde{v}_f$ profile is characterized by some resemblance to the $\widetilde{U}_{xf}$ amplitude, while in the region placed further downstream (see Fig.4b,c) the $\widetilde{v}_f$ temperature component is rather under the influence of radial amplitude $\widetilde{U}_{rf}$ of the periodical motion. The explanation of the above observation is presented by Elsner et al (1989a), who has found that the initial region of the jet is dominated by longitudinal oscillating and the $\widetilde{v}_f$ profile in Fig.4a may support this statement. In the region $x/D > 1.5$ the radial transport of heat prevails and that is why the distributions of $\widetilde{v}_f$ in Fig.4b,c are under the influence of $\widetilde{U}_{xf}$ component.

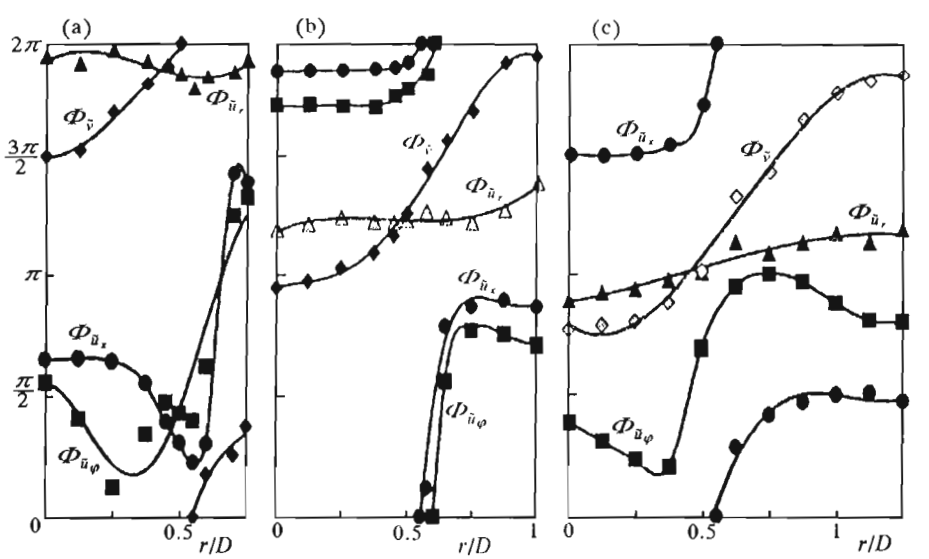

Fig. 5. Radial distributions of the fundamental harmonics phase angles for the oscillatory components of velocity and temperature at the cross-sections: (a) – $x/D = 1.5$, (b) – $x/D = 2.5$, (c) – $x/D = 4.0$

Another important characteristics of the coherent vortex is the distribution of phase angles of particular oscillatory amplitudes shown in Fig.5 and calculated relative to the acoustic pressure, which was treated as a phase-reference signal. The profiles of the phase angle for the longitudinal velocity component $\Phi_{\widetilde{U}_x}$ reveal a phase shift $\sim \pi$ near the $r/D = 0.5$ line, the presenting the trajectory of vortex centre. One should also notice that in the inner and outer regions, respectively, of the jet the phase angle $\Phi_{\widetilde{U}_x}$ is almost constant. Very similar is the behaviour of the phase angle of circumferential velocity component $\Phi_{\widetilde{u\phi}}$, while the $\Phi_{\widetilde{U_{ur}}}$ phase angle is nearly constant across the whole jet radius in the cross-sections analyzed. All the above observations confirm that the coherent structures existing in the initial region of the jet mixing layer have the structures similar to those of free potential vortices.

The phase angle $\Phi_{\widetilde{v}}$ of the temperature oscillatory component changes gradually within the range $(0, \pi)$ across all cross-sections (see Fig.5) without any sudden change in the vicinity of the vortex centre. Such a behaviour of $\Phi_{\widetilde{v}}$ may be interpreted (cf Favre-Marinet and Binder (1987), Favre-Marinet (1989)) as a result of the interaction of small scale turbulence with the oscillatory temperature field.

4. Propagation of the coherent vortex in the jet mixing layer

The coherent vortex during its spatial development travels downstream at a pace different from the velocity of mean flow, which in turn implies a complex distortion of the flow field analyzed. That is why the experimental determination of convection velocity is in general a complex problem, the more so if one takes into account the fact that the coherent structures continously change their shape, size and orientation, due to the presence of random turbulence. A large number of different measuring techniques have been developed for this purpose, starting from simple oscilloscope observations of the signals from the stationary and moving hot-wire probes (e.g. Paschereit et al. (1992)) to more complex correlation techniques (cf Drobniak (1986)). If the flow is externally stimulated, then the convection velocity U_c may be calculated from the time-courses of the oscilatory longitudinal velocity component $\widetilde{U}_x(t)$ measured at auxiliary plane placed at a distance Δx using the formula

$$U_c = \frac{2\pi \Delta x}{T \Delta \phi} \tag{4.1}$$

where

$\Delta\phi$ – phase-shift angle between the two $\tilde{U}_x(t)$ courses measured at some radial distance in two consecutive planes separated by the streamwise distance Δx.

On the one hand the distance Δx between the main and auxiliary planes (see Fig.2) should be sufficiently small in comparison with the wavelength λ_s of the column-mode structures and, on the other hand it should be large enough to enable the accurate estimation of convection velocity. The analysis of data collected during the preliminary measurements (cf Elsner et al. (1989b)) as well as the estimates obtained by Favre-Marinet (1989) allowed us to select the value $\Delta x/\lambda_s = 0.08$ (i.e. $\Delta x/D = 0.125$) as an acceptable compromise.

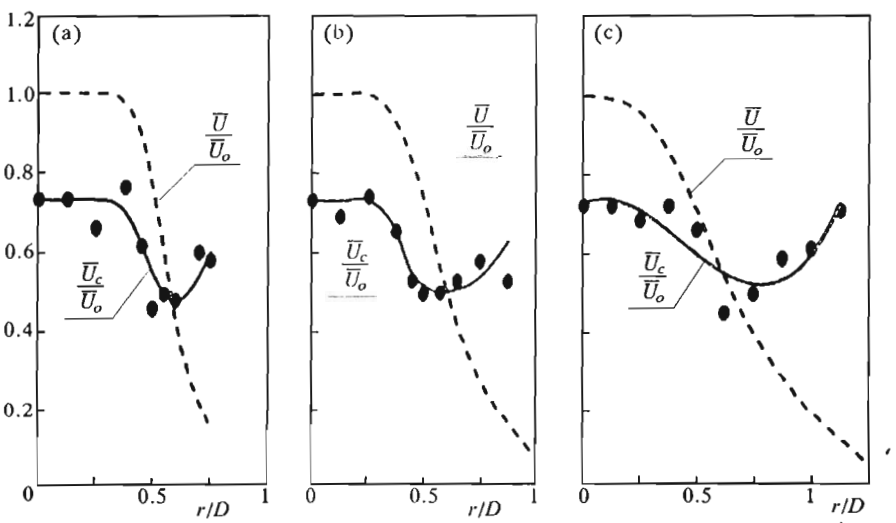

Fig. 6. Radial distributions of the time-mean $(\overline{U}_x/\overline{U}_o)$ and convection $(\overline{U}_c/\overline{U}_o)$ velocities at the cross-sections: (a) – $x/D = 1.5$, (b) – $x/D = 2.5$, (c) – $x/D = 4.0$

The results of $U_c(r)$ calculations have been presented in Fig.6 together with the corresponding mean velocity distributions $\overline{U}_x(r)$ for the three main cross-sections, respectively. One may notice the uniform U_c profile inside the potential core, while outside the core the convection velocity decreases, taking the $U_c/U_o \cong 0.5$ value at the centre of vortex ($r \approx r_{0.5\overline{U}}$) and at $x/D = 1.5$ and $x/D = 2.5$ cross-sections, respectively. The higher value $U_c/U_o \cong 0.6$ at the $r = r_{0.5\overline{U}}$ line for $x/D = 4$ (see Fig.6c) suggests acceleration of the vortex centre, when a gradual decay of the structure begins. At first, the non-uniform radial distribution of U_c may indicate the change of orientation of the coherent vortex, resulting in gradual tilting of its principal axis as it

has been suggested by Hussain and Zaman (1980). Furthermore, the decay of coherent structure which is most serious in the outer part of the jet (cf El-Sayed El-Kassem (1995)), results in the development of smaller-scale vortices which travel faster than the large-scale ones (cf Wygnanski and Fiedler (1969)). That is the reason, why the profile of convection velocity becomes more flat when the point of observation is being moved downstream. As a result, the growing fraction of smaller vortices reflects on a higher mean value of U_c observed in the $x/D = 4$ cross-section in comparison with the previous ones.

5. The "frozen" flow field characteristics of the coherent vortex

The organized motion present in the flow considered, was understood as "coherent vortices" mainly on the basis of observations of oscilloscope traces presenting the time-courses of temperature and particular velocity components. The characteristic distributions of root-mean-square values as well as the profiles of fundamental amplitudes of the velocity and temperature fields could be treated as supplementary proofs of the vortex character of the organized structures. However, it seems necessary to have the quantitative data that could support the idea that the organized motion may be regarded as a chain of repetitive vortices developing in the mixing layer. That is why it has been decided to perform a computer extraction of the periodic motion, that would enable one to reconstruct the flow field picture, as if it was seen by an observer moving with the structure. The centre of vortex has been selected as the best location of the observer and the average convection velocity $\widehat{U}_c$ has been chosen to be the velocity of the moving observer. The Taylor hypothesis has been accepted locally for each main cross-section; i.e., $x/D = 1.5$, 2.5 and 4, respectively. The non-dimensional longitudinal coordinate, calculated as

$$\frac{\Delta x}{D} = -\widehat{U}_c \frac{\Delta t}{D}$$

where Δt is the time step of calculations has been adjusted properly to locate the centre of vortex in the middle of each picture. The length of the picture has been properly scaled to accomodate approximately one wavelength of the structure, which in the case of the present experiment was equal to $\lambda_s \cong 1.55D$. The $\Delta x/D = 0$ coordinate at all consecutive pictures denotes the $t/T = 0$ time of phase-averaging beginning (i.e. the positive zero-crossing of the phase-reference signal). The radial r/D and longitudinal $\Delta x/D$ coordinates, respectively, have been drawn in the same scale to enable

an easier comparison of the shape of coherent structure as it passes across a particular cross-section.

The quantitative conclusions about the structure of the vortex may be drawn from Fig.7 and Fig.8, presenting the isoline contours of non-dimensional phase-averaged longitudinal $\langle U_x \rangle / \overline{U}_o$ and radial $\langle U_r \rangle / \overline{U}_o$ velocity components, respectively.

As may be noticed in Fig.7, the region of maximum values of $\langle U_x \rangle$ shifts gradually towards the jet axis, when the point of observation is being moved downstream. Furthermore, the highest amplitudes of $\langle U_x \rangle$ are encountered at the $x/D = 2.5$ plane (Fig.7b and Fig.8b), where the coherent vortex reveals its maximum spatial coherence, and the most regular patterns of both $\langle U_x \rangle$ and $\langle U_r \rangle$ isolines may be observed. As can be seen from Fig.8, the vortex moving from the left to the right of the picture appears at its front the area of positive $\langle U_r \rangle$ amplitudes, which may be attributed to the existence of the outward radial stream (i.e. directed from the jet axis to the outer jet boundary). The negative $\langle U_r \rangle$ values observed in Fig.8 at the rear side of vortex correspond to the areas of radial transport directed towards the jet axis. The zero $\langle U_r \rangle$ isoline, which forms a saddle between the areas of positive and negative values of $\langle U_r \rangle$, respectively, is inclined at an angle smaller than $\pi/2$ to the jet axis in the initial jet region (see Fig.8a). As the vortex moves downstream the zero $\langle U_r \rangle$ isoline becomes vertical (Fig.8b) and then (in the last cross-section analyzed) it inclines to the jet axis at an angle higher than $\pi/2$ (Fig.8c). This observation proves the gradual deformation of the vortex shape, which takes place during its movement in the down-stream direction, which results from the non-uniform radial distribution of the vortex convection velocity.

More detailed information about the internal structure of the vortex may be obtained from the analysis of isoline contours of non-dimensional longitudinal velocity component $\tilde{u}_x / \overline{U}_o$ of oscillating in Fig.9 for the same three cross-sections. Since $\overline{U}_r$ is relatively small, the isoline contours of $\tilde{u}_r$ are not very much different from the phase-averaged radial velocity component $\langle U_r \rangle$ (Fig.8) and were not presented here. The results presented in Fig.9 demonstrate that the peaks of both the maximum and minimum values of $\tilde{u}_r$ are being shifted towards the jet axis when the vortex moves downstream. At the same time one may notice the asymmetry of $\tilde{u}_r$ contours with respect to the trajectory of the vortex centre (i.e. the $r/D \approx 0.5$ line) because the absolute values of $\tilde{u}_r$ in the inner area of the jet are at least one order of magnitude smaller than those in the outer region. One may conclude therefore, that the spatial coherence of the structure is preserved much better on the high velocity side of the mixing layer. The resultes of present experiment reveal the evident similarity (both qualitative and quantitative) with those of Hussain

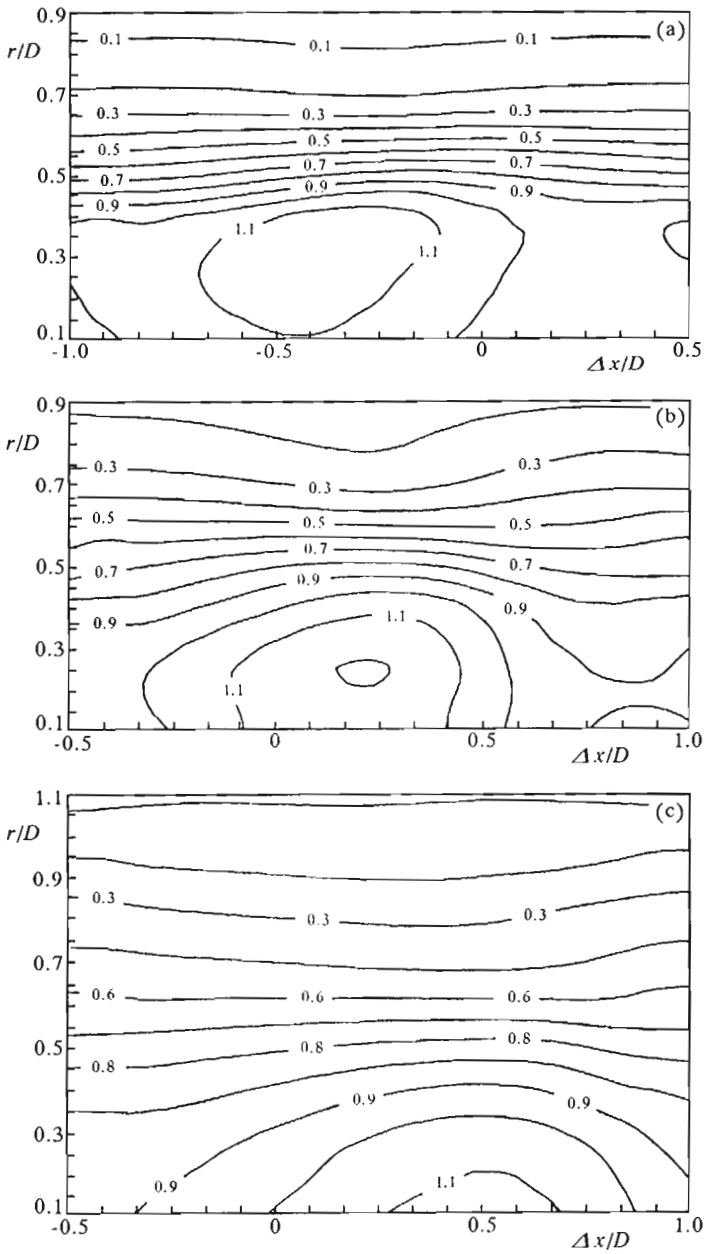

Fig. 7. Isoline contours of the phase-averaged longitudinal velocity component $\langle U_x \rangle / \overline{U}_o$ at the cross sections: (a) - $x/D = 1.5$, (b) - $x/D = 2.5$, (c) - $x/D = 4.0$

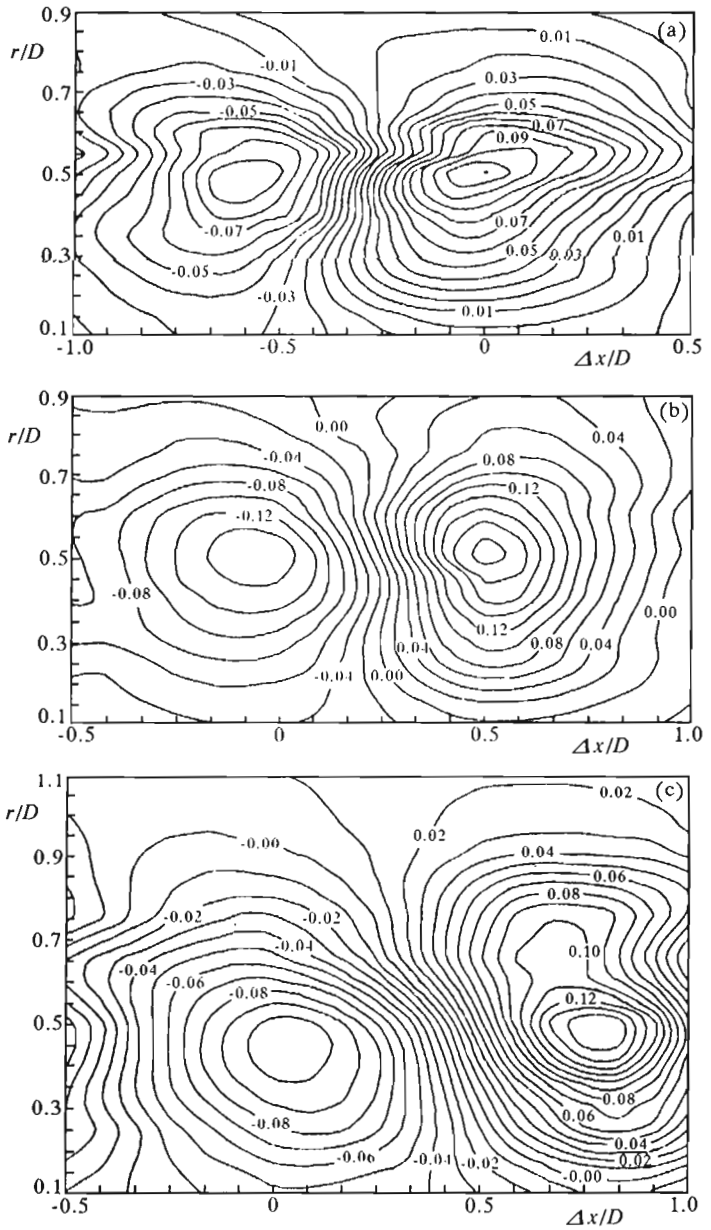

Fig. 8. Isoline contours of the phase-averaged radial velocity component $\langle U_r \rangle / \overline{U}_o$ at the cross sections: (a) – $x/D = 1.5$, (b) – $x/D = 2.5$, (c) – $x/D = 4.0$

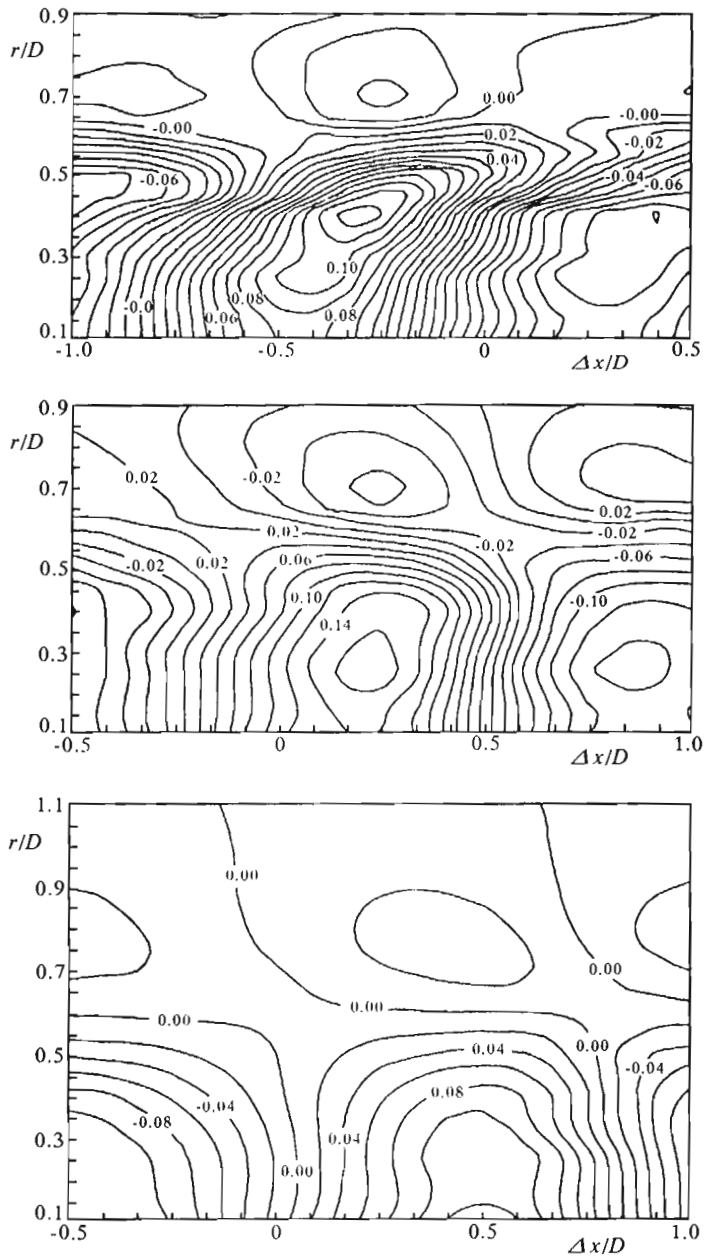

Fig. 9. Isoline contours of the longitudinal oscillatory velocity component $\widetilde{u}_x/\overline{U}_o$ at the cross sections: (a) – $x/D = 1.5$, (b) – $x/D = 2.5$, (c) – $x/D = 4.0$

and Zaman (1980), where the structure of coherent vortex has been deduced from the records taken simultaneously at a large number of points distributed uniformly over the whole area analyzed. As in the latter case there was no need to apply the Taylor hypothesis, so bearing in mind the correspondence mentioned above, one may conclude that the use of Taylor hypothesis is quite permissible for a column-mode structure, which are not subjected to sudden deformations like pairing or tearing.

A valuable information about the vortex internal structure may also be obtained from the non-dimensional phase-averaged temperature isoline contours $\langle\Theta\rangle/\Delta\overline{\Theta}_o$ presented in Fig.10. The shape of $\langle\Theta\rangle/\Delta\overline{\Theta}_o$ isolines suggests clearly, that the front side of vortex transports the hot air from the potential core to the outer boundary of the jet, while at the rear side of the coherent structure the cool ambient air is transferred towards the jet axis. Even more illustrative are the spatial distributions of the non-dimensional periodical temperature component $\tilde{v}/\Delta\Theta_o$ isolines, presented in Fig.11 for all the cross-sections considered. The highest values of $\tilde{v}$ may be observed at the plane $x/D = 2.5$ (Fig.11b) that suggests the convective nature of heat transfer processes realized by the coherent vortex, because at this very plane the maximum amplitudes of oscillatory velocity components may be observed. The distributions of $\tilde{v}$ isoline contours presented in Fig.11 prove, that both the hot air stream ejected from the potential core and the cool ambient air stream entrained into the jet core are inclined backwards at an angle equal $\sim \pi/4$ to the direction of jet axis. These results prove quantitatively the existence of typical "wedge" structures for which the qualitative evidence has been given in the previous Schlieren visualizations (cf Yule (1978)). The interesting feature is, that all these conclusions could be drawn from the analysis of isoline patterns characterizing the temperature field, then from the velocity ones. Thus the temperature field may be regarded as a sensitive indicator of the internal structure of coherent vortex, that confirms the validity of the main assumptions applied in the present experiment.

6. Conclusions

The computer-aided signal processing techniques applied in the present experiment allowed us to obtain the description of the internal structure of coherent vortices existing in the initial region of a round free jet. The phase averaging procedure and computer visualization methods based on the analysis of velocity and temperature signals, aided by the Taylor hypothesis proved to

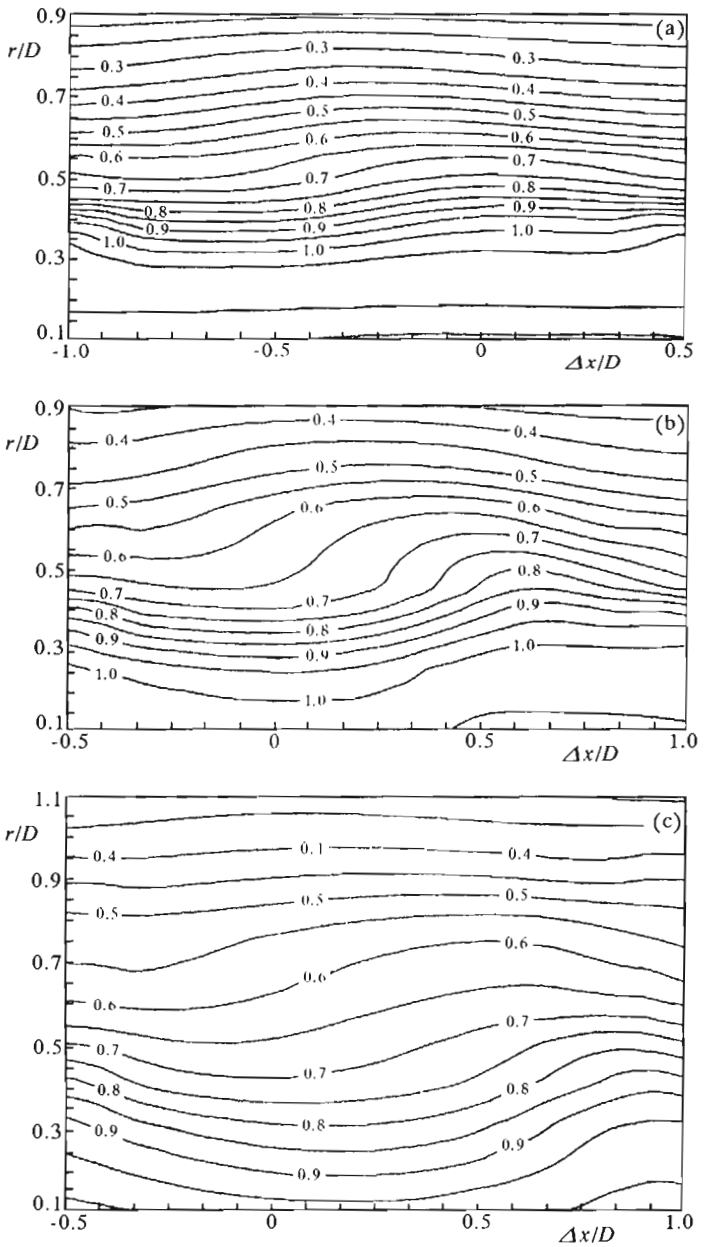

Fig. 10. Isoline contours of the phase-averaged temperature $\langle\Theta\rangle/\Delta\overline{\Theta}_o$ at the cross sections: (a) – $x/D = 1.5$, (b) – $x/D = 2.5$, (c) – $x/D = 4.0$

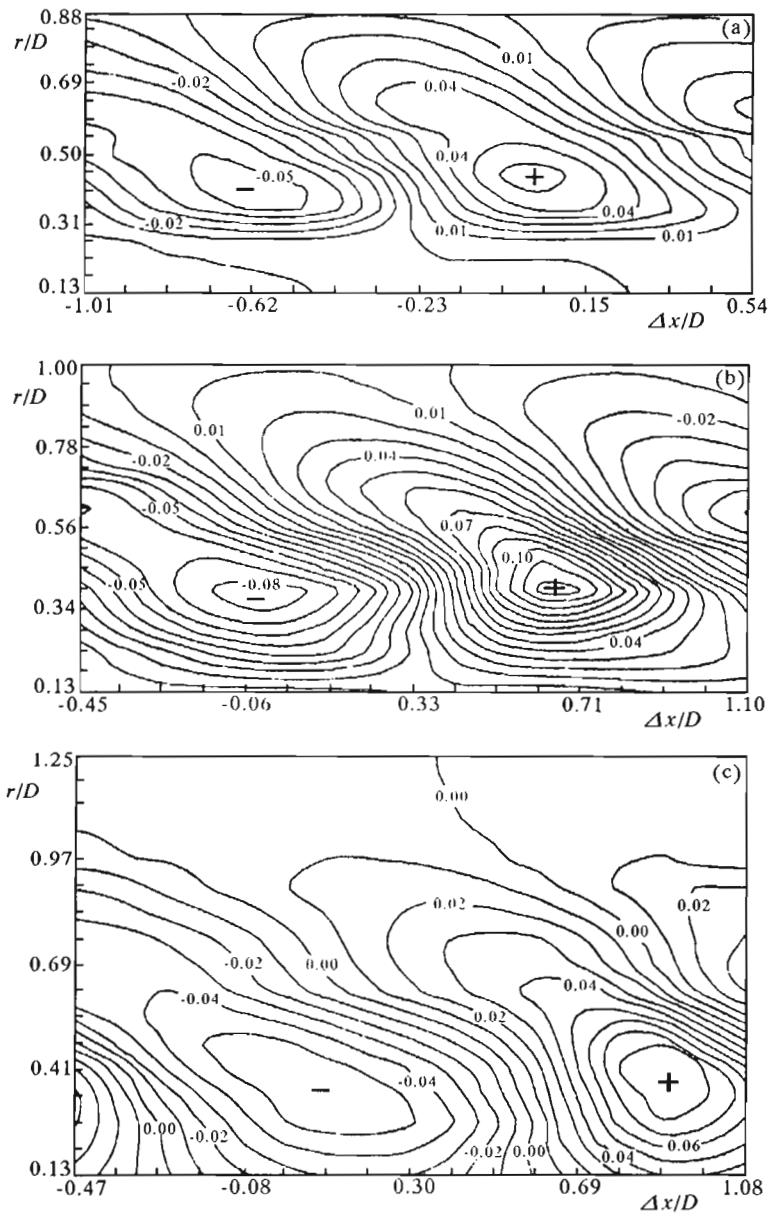

Fig. 11. Isoline contours of the oscillatory temperature component $\tilde{v}/\Delta\Theta_o$ at the cross sections: (a) – $x/D = 1.5$, (b) – $x/D = 2.5$, (c) – $x/D = 4.0$

be an effective tool for reconstruction of the flow patten of coherent motion. The column-mode coherent structures developing in the initial region of the jet mixing layer appeared to be the classical potential vortices, at least, at the beginning of their formation. The vortex flow field is closely related to the intensity of transport processes realized in the flow considered because the front side of the vortex transports the air from the potential core to the outer jet boundary, while at its rear side the ambient air is entrained towards the jet axis.

At the next stages of structure formation, the centres of vortices are shifted gradually towards the jet axis and the change of vortex orientation may be observed, because the symmetry lines of vortex cores become more tilted towards the jet axis. The above deformation stems from the non-uniform distribution of convection velocity and as a result, the air streams transported by the vortex become inclined backwards, and the typical wedge structure may be observed in the futher distance from the exit. The coherence of the potential vortices is lost much faster in the outer region of the jet what leads to the increase of convection velocity. The distinct relation between the amplitudes of oscillatory components of velocity and temperature as certains the convective nature of heat transport processes encountered in the initial region of the round, free jet. The above observations suggest therefore, that the coherent structures of the round, free jet are initially the potential vortices, then subjected to complex deformations, which in turn finds its reflection in the intensity of transport processes realized in the flow considered.

Acknowledgments

The authors acknowledge support of the State Committee for Scientific Research under Grant No. 7T07C005008.

References

1. CROW S.C., CHAMPAGNE F.H., 1971, Orderly Structure in Jet Turbulence, *J. Fluid Mech.*, **48**, 547-591

2. DROBNIAK S., 1986, *Struktury koherentne swobodnej strugi osiowosymetrycznej*, Pol.Częstochowska, Seria Monografie, Nr 1

3. DROBNIAK S., ELSNER J.W., 1986, Coherent Structures and their Relation to Instability Processes in a Round, Free Jet, *Adv. in Turbulence*, Springer-Verlag

4. EL-SAYED K.A.EL-KASSEM, 1995, An Analysis of Heat Transfer Processes in the Coherence Region of a Round, Free Jet, Ph.D. Thesis, Pol. Częstochowska

5. ELSNER J.W., DROBNIAK S., KŁAJNY R., ZIELIŃSKI J., 1987, Computer Aided Method for Solving Instantaneous Hot-Wire Response Equations in a Plane Non-Isothermal Flows, *Arch. Termodynamiki*, **8**, 4, 309-324

6. ELSNER J.W., DROBNIAK S., KŁAJNY R., 1989a, Behaviour of Column-Mode Vortex Structures in the Near-Flow Region of a Round, Free Jet, *Turbulence*, **1**, 35-50

7. ELSNER J.W., DROBNIAK S., KŁAJNY R., 1989b, Formation of Helical Structures in a Round, Free Jet, *Adv. in Turb.*, **2**, Springer-Verlag

8. ELSNER J.W., DROBNIAK D., KŁAJNY R., 1992, Contribution of Coherent Structures to Heat and Mass Transport in the Round, Free Jet, *Proc. V Symp. on Heat and Mass Transfer*, Białowieża, 149-156

9. ELSNER J.W., DROBNIAK S., KŁAJNY R., 1993, An Analysis of Energy Transport Processes in the Presence of Coherent Structures, *Adv. in Turbulence* IV, Kluwer Acad.Publ.

10. FAVRE-MARINET M., 1989, Coherent Structures in a Round Jet, *Proc. von Karman Inst. for Fluid Dynamics*, Lecture Series, 1989-03

11. FAVRE-MARINET M., BINDER G., 1987, Amplification and Decay Mechanisms of Coherent Structures in a Round Jet, *Proc. VI Symp. Turb. Shear Flows*, Tolouse

12. HUSSAIN A.K.M.F., 1986, Coherent Structures and Turbulence, *J. Fluid Mech.*, **173**, 303-356

13. HUSSAIN A.K.M.F., ZAMAN K.B.M.Q., 1980, Vortex Pairing in Circular Jet under Controlled Excitation, Pt. 2, Coherent Structure Dynamics, *J. Fluid Mech.*, **101**, 3, 493-544

14. PASCHEREIT C.O., OSTER D., LOND T.A., FIEDLER H., WYGNANSKI I., 1992, Flow Visualization of Interaction among Large Coherent Structures in an Axisymmetric Jet, *Exp. in Fluids*, **12**, 189-199

15. WYGNANSKI I., FIEDLER H., 1969, Some Measurements in the Self-Preserving Jet, *J. Fluid Mech.*, **38**, 3, 577-612

16. YULE A.J., 1978, Large-Scale Structure in the Mixing Layer of a Round Jet, *J. Fluid Mech.*, **89**, 3, 413-432

Struktura wewnętrzna koherentnego wiru w osiowo-symetrycznej strudze swobodnej

Streszczenie

Praca poświęcona jest analizie własności kinematycznych struktury koherentnej typu "modu kolumnowego" występującej w początkowym obszarze swobodnej strugi kołowej. Zastosowanie technik komputerowego wspomagania eksperymentu pozwoliło na rekonstrukcję pola prędkości wewnątrz koherentnego wiru umożliwiając również wykazanie, że struktury koherentne intensyfikują w sposób istotny procesy transportu w analizowanym przepływie. Uzyskane wyniki wskazują, że w początkowej fazie rozwoju kinematyka wiru koherentnego jest w zasadzie identyczna z potencjalnym pierścieniem wirowym. Niejednorodny wzdłuż promienia strugi profil prędkości

konwekcji powoduje natomiast, że w miarę oddalania się od wylotu z dyszy koherentny pierścień wirowy podlega deformacji, w wyniku której oś symetrii rdzenia wiru przestaje być równoległa do osi strugi. Dodatkowo, działanie sił lepkości powoduje, że zewnętrzny obszar struktury wirowej traci spójność fazową, a powstające w wyniku rozpadu struktury koherentnej wiry o małych skalach wywołują wzrost prędkości konwekcji w zewnętrznej strefie strugi. Analiza wzajemnych przesunięć fazowych między oscylacyjnymi składowymi prędkości i temperatury pozwoliła wykazać istnienie ścisłego związku między polem prędkości w obszarze koherentego wiru a intensywnością realizowanego przezeń transportu ciepła.

Manuscript received December 5, 1996; accepted for print January 22, 1997